Experimental and numerical study of natural convection in 3D double horizontal annulus

Jan Pařez[1*], *Adam* Tater[2], *Jiří* Polanský[3], and *Tomáš* Vampola[1]

[1]Department of Mechanics, Biomechanics and Mechatronics, Faculty of Mechanical Engineering, Center of Advanced Aerospace Technology, Czech Technical University in Prague. Technicka 4, Praha 6, Czech Republic.
[2]Department of Technical Mathematics, Faculty of Mechanical Engineering, Center of Advanced Aerospace Technology, Czech Technical University in Prague. Technicka 4, Praha 6, Czech Republic.
[3]Department of Fluid Dynamics and Thermodynamics, Faculty of Mechanical Engineering, Czech Technical University in Prague. Technicka 4, Praha 6, Czech Republic.

Abstract. Presented paper is focused on numerical simulation of turboprop engine cooling in the section of a gas turbine. The method of heat transfer motor cooling by natural convection and radiation is described. The heat transfer in gas turbine section is represented on a simplified double annular geometry. Numerical data were compared with data that was gained from measuring on an experimental stand. The surface temperatures of the tubes were measured on the experiment stand during the cooling of the engine model. Numerical and experimental results reach a good agreement and will be further applied to the study of temperature-dependent deformation of aircraft engine parts, which have a significant effect on the safety and flawless operation of the aircraft engine.

1 Introduction

After the running turboprop engine is turned off, the engine is started to cooling down spontaneously. This cooling is not symmetrical due to natural convection. Due to the lower density, the hot gases rise upwards, resulting in a different temperature gradient between the upper and bottom side. The upper half of the engine parts are hotter and thus have lower heat transfer than the bottom part of the section (Neely and Smith [1]). Heat transfer due to natural convection in a simple 2D annulus has been described in numbers of papers with several approaches. (Yang and Kong [2], Zubkov and Narygin [3], Abu-Nada et al. [4], Francis et al. [5]). Natural convection in a circular enclosure with an internal polynomial cylinder geometry was studied in (Wang et al. [6]), on top of this, non-eccentric heat transfer due to natural convection was presented in (Prusa and Yao [7]).

A more complex phenomenon occurs when considering cooling in the generator turbine section of a turboprop engine. The turbine section of a turboprop engine consists of a double intermediate ring, where the inner intermediate ring corresponds to the flow path of the hot flue gases and the outer intermediate ring corresponds to the separation of the flow path from the engine case. The indicated scheme of the solved area is shown in Fig. 1.

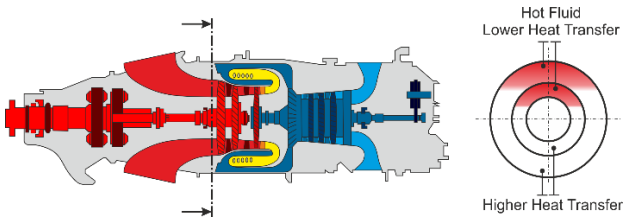

Fig. 1. Solving area of turboprop engine.

In the case of a double annulus, similarly to the simple model of the annulus, natural convection occurs when the engine is cooling down. The inner section of the flow path is asymmetrically cooled in the same time the outer section is asymmetrically heated from the hot gases of the inner section of the flow path, this asymmetry is caused by heat transfer of natural convection and radiation. In previous research, a 2D model of heat transfer caused by natural convection and radiation in a double annulus based on measuring data was presented [8].

This research has been simplified to a 2D model which does not include the effect of vorticity from natural convection and heat transfer by heat conduction in tubes. In (Padilla and Silveira-Neto [9], Krishnayatra et al. [10]) the 3D effect of natural convection is presented.

The presented paper presents a numerical study of cooling due to natural convection in a double annulus and heat transfer by radiation with an S2S model based on the geometry and boundary conditions of a turboprop engine. The geometry is showed in Fig. 2 and

* Corresponding author: jan.parez@fs.cvut.cz

corresponds to the simplification of the turbine section of the turboprop engine in Fig. 1. The initial conditions were chosen to be the constant temperature for the partially solved areas. Subsequently, there is the development of natural convection and heat transfer by radiation. Conditions are based on real measured temperature data on the running engine, which were presented in previous research (Solnař et al. [11]). Chosen models of S2S radiation and heat conduction by conduction through the tubes according to Fig. 2. Tubes thicknesses and tubes dimensions correspond to a simplification of the gas turbine. The values of the course of temperatures by the numerical model were further compared with experimental measurements on a measuring stand.

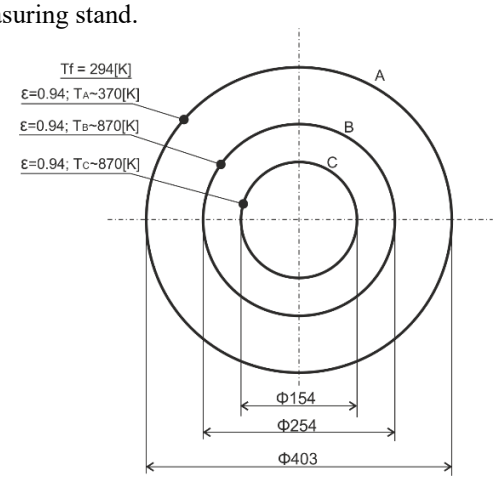

Fig. 2. Simplification sketch of generator turbine geometry.

2 Numerical model

Natural convection is very important in many engineering applications. With a suitable model it is possible to predict the flow caused by natural convection in a turbine engine. This makes it possible to influence temperatures and temperature fields when developing the engine.

The numerical model in Ansys Fluent software for natural convection and heat radiation are presented in this chapter. The conservation equations of mass, momentum and energy of fluid are considered.

A transient pressure-based coupled solver is used. Spatial discretization methods for pressure, momentum and turbulent properties are chosen as second order accurate. Time discretization is chosen as second order accurate implicit method with iterative time stepping. Air is modelled as incompressible-ideal-gas which density is defined as

$$\rho = \frac{p_{op}}{rT}, \tag{1}$$

where p_{op} is the operational pressure which is considered atmospheric, r is the specific gas constant and T is thermodynamic temperature. This model is recommended by Ansys for cases of natural convection with high temperature gradients. Moreover, specific heat is considered as piecewise-polynomial function. Thermal conductivity is assumed constant and viscosity is modelled by Sutherland's relation. Turbulence is modelled by k-omega SST model with additional transport equation for intermittency providing transition of laminar flow to turbulent. This turbulent flow solver must be further coupled with S2S radiation model with prescribed emissivity values described in Fig. 2. as radiation is the prevailing phenomenon in the beginning of the simulations. Initial values are constant temperatures for individual tubes. In fluid regions, gauge pressure is set to zero, temperature is considered standard atmospheric. Velocity in each fluid region is set to near zero value. Turbulence initial values correspond to previously mentioned values and characteristic length of computational domain. Boundary conditions on front and back faces are set as adiabatic no-slip walls. Walls that connect fluid regions with solid tubes are set to coupled no-slip walls. Heat transfer between the atmosphere and the outer surface of the largest tube is modelled by average heat transfer coefficient, defined in [12], which is variable throughout the simulation. Our transient simulations are performed until 45 minutes of real time from the start of the process. Time step length is constant and set to one second with 50 inner iterations. This prevents the Courant number to exceed 200 throughout the simulation. Computational mesh is a high quality, fully structured grid with nearly 2 million cells. The numerical method is then validated by comparing numerical results with experimental results from measurements.

The usage of turbulence models decides the „expected“ flow regime in the solved geometry. In case of problems with natural convection, Rayleigh's number Eq. 2 determines the flow regime [13]. Let us informally estimate the value of the Rayleigh's number in the case of natural convection around the middle surface of the annulus.

$$Ra = \frac{\beta g \Delta T L^3}{v^2} Pr \tag{2}$$

where is used the middle diameter (ø254 mm) of the annulus as a characteristic dimension, see Fig. 2, and the air properties at the temperature difference of 580 [°C]. The calculated value of Rayleigh's number is 10^7. This value is in turbulent flow regime in natural convection. The showed numerical model is applied to the natural convection in a horizontal double concentric cylindrical tube with Rayleigh number in the range of 10^7 to 10^3 and Prandtl number in the range of 0.01 to 10. (Yang and Kong [14]).

In general, the flow is laminar at low Rayleigh number but turbulent at high Rayleigh number. The transition Rayleigh number from stable to unstable states is lower in the low Prandtl number cases than in the high Prandtl number cases.

In the following figures Fig. 3 to Fig. 8 is shown the temperature field affected by cooling due to natural convection and thermal radiation in a double concentric annulus. The first Fig. 3 is showed the temperature field after 15 minutes of cooling. The second Fig. 4 is shown after 30 minutes, Fig. 5 is after cooling for 45 minutes. There is a noticeable temperature difference between the top and bottom of the double annulus causing the temperature difference.

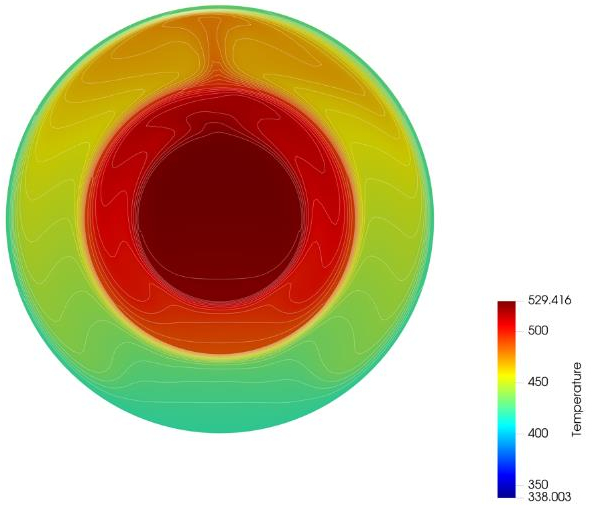

Fig. 3. Temperature field after 15 minutes.

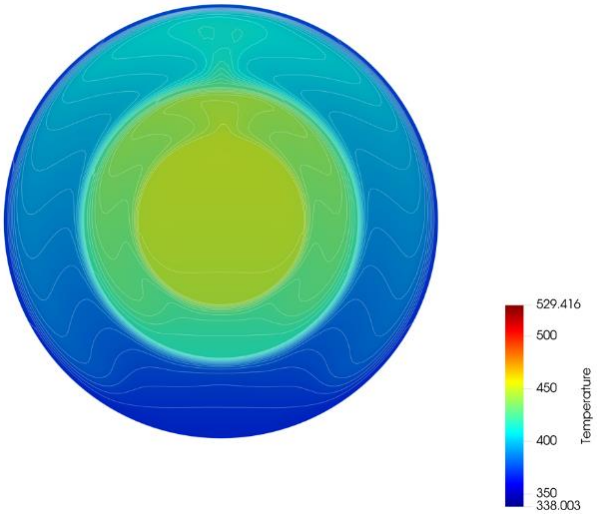

Fig. 4. Temperature field after 30 minutes.

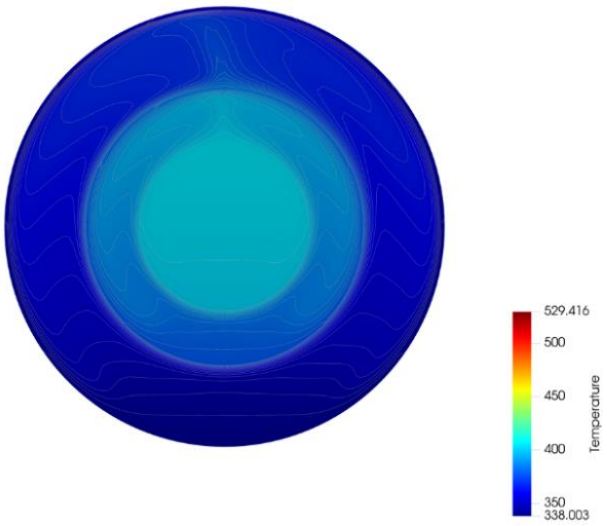

Fig. 5. Temperature field after 45 minutes.

On Fig. 6 to Fig. 8 is shown an identical temperature field in three perpendicular planes.

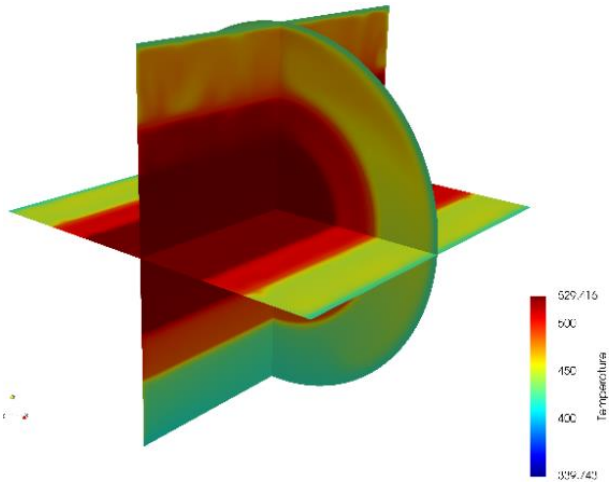

Fig. 6. Temperature field after 15 minutes.

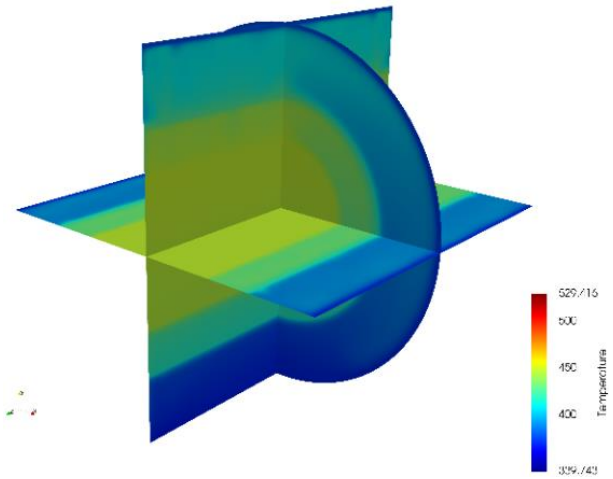

Fig. 7. Temperature field after 30 minutes.

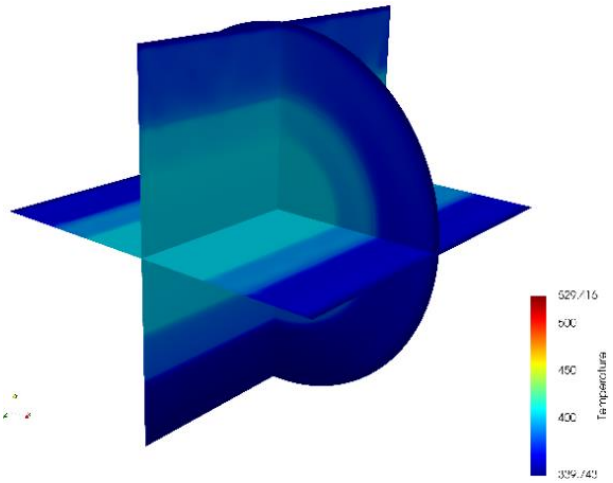

Fig. 8. Temperature field after 45 minutes.

The velocity field during natural convection due to the temperature-dependent change in density is shown in the following Fig. 9 to Fig. 11.

The flow is mainly at the walls of the tubes. This is due to the rotational circulation of air, where the hot air flows through the inner wall of the respective area of the annulus, where the air is further heated. The hot stream is then torn off the wall and forms a hot plumes. It flows upwards where it hits the upper wall and is pulled down by the cooler wall at the bottom of the wall.

The Rayleigh-Bénard Convection effect is noticeable in the flow. (King et al. [15]) studied this phenomenon in his works.

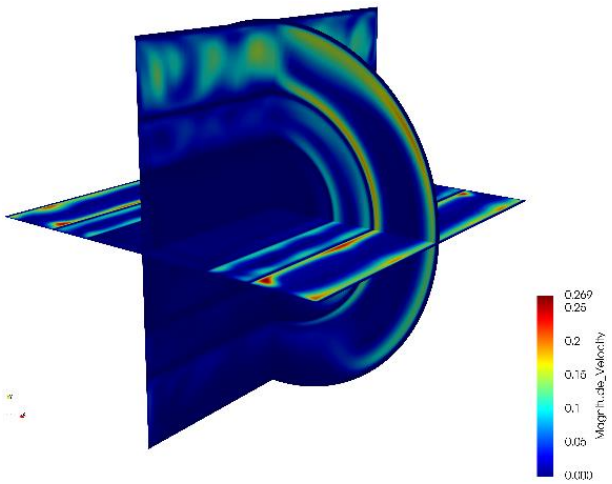

Fig. 9. Velocity field after 15 minutes.

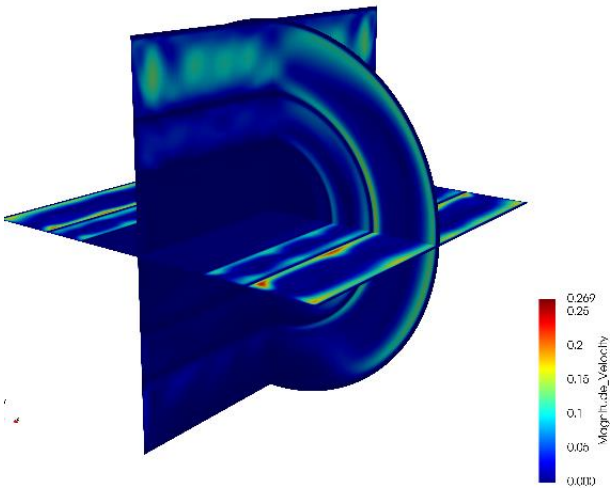

Fig. 10. Velocity field after 30 minutes.

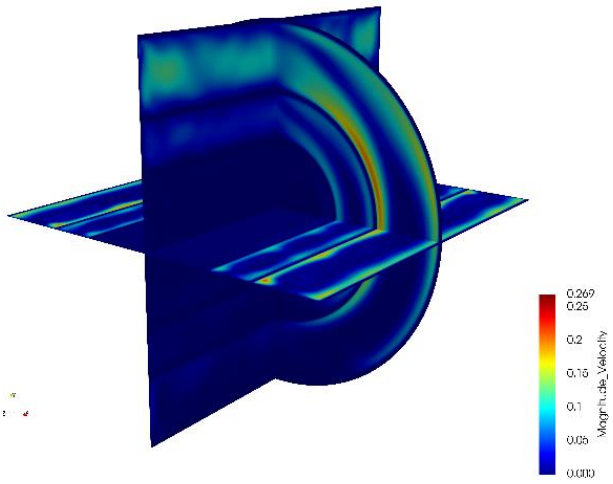

Fig. 11. Velocity field after 45 minutes.

The graph in Fig. 12 shows a convergence analysis of the solved mesh of the model. The trend of convergence shows that when using a solving mesh over 1 million elements, a sufficient deviation is achieved exceeding the range of thermocouple measurements on the experimental stand located according to Fig. 13.

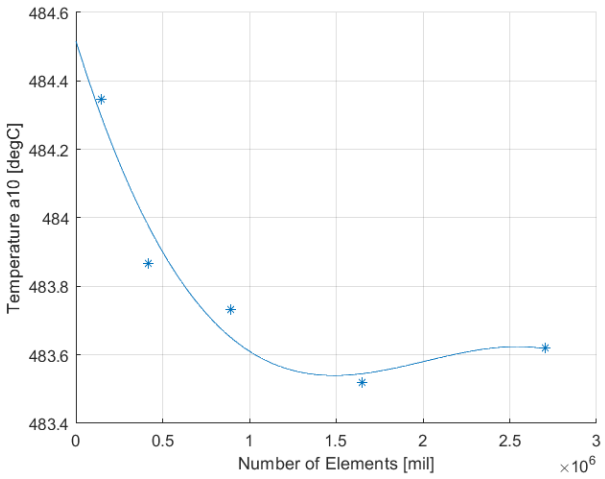

Fig. 12. Convergence analysis of the solved mesh of the model.

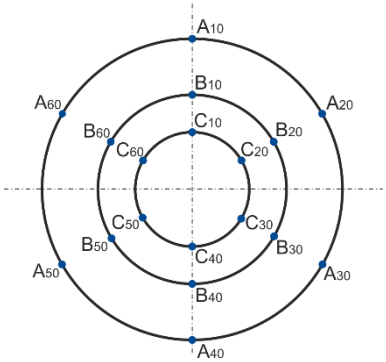

Fig. 13. Placement of K-Thermocouples on a double annulus.

3 Comparing of the numerical model on the measured data

3.1 Measuring stand Design

To verify the accuracy of the numerical model and its assumptions, an experimental stand was designed, where the visualization is showed on Fig. 14. The design of the stand is based on the geometry of the turboprop engine on Fig. 2 and is unified with a numerical model. The measuring section consisting of concentric tubes is mounted on a base frame. The front and rear sides are covered with isolated covers, in which the clearance is monitored and direct contact with the tubes is prevented. The measuring section is insulated from the covers and the base by ceramic high-temperature insulation Tyrasil made of ceramic fibres. This prevents heat transfer outside the measuring space.

Fig. 14. Visualization of measuring stand.

3.2 Instrumentation

The measuring stand is instrumented with heating elements for tempering to the required temperature and measuring thermocouples for measuring the temperature field. The flow path of the inner and middle tubes is heated by a Dawell resistance heater.

The temperature field was measured in three equidistant planes on each tube. Furthermore, the measurements in each plane were divided into 6 equivalent spaced K-Thermocouples on each tube shown in Fig. 13. This is a total of 54 K-Thermocouples for measuring the temperature field on tubes. Finally, 3 thermocouples were installed to record the course of heating temperatures. On the Fig. 15 and Fig. 16 is showed the measurement on the measuring stand. The Fig. 15 shows the analysis with a Flir thermal camera.

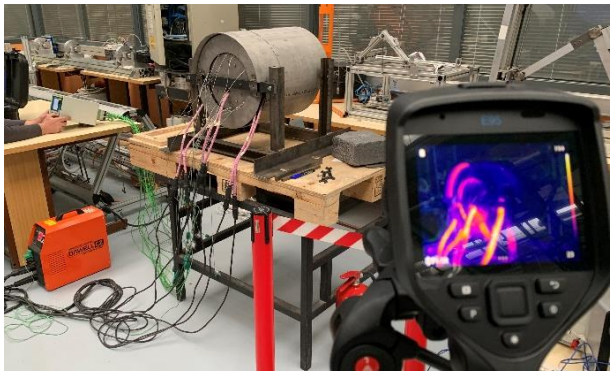

Fig. 15. Analysis by Flir thermal camera.

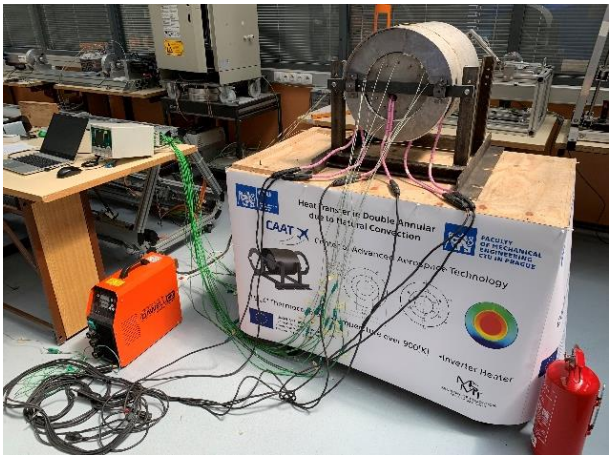

Fig. 16. Experimental measuring on the stand.

3.3 Validation

The numerical model was validated to verify they reach an agreement of the considered initial conditions and boundary conditions presented in the chapter of numerical calculation. By comparing the data obtained on the basis of experimental measurements with data from the numerical model, the waveforms and values of the temperature field during cooling of the computational model were compared as shown on Fig 17 to Fig. 19. Each curve corresponds to the location of the thermocouple in Fig. 13, where the highest temperature is at the upper point marked A10 and further descending to the point with the lowest temperature at A40. A similar temperature profile applies to other tubes on Fig. 18 and Fig. 19.

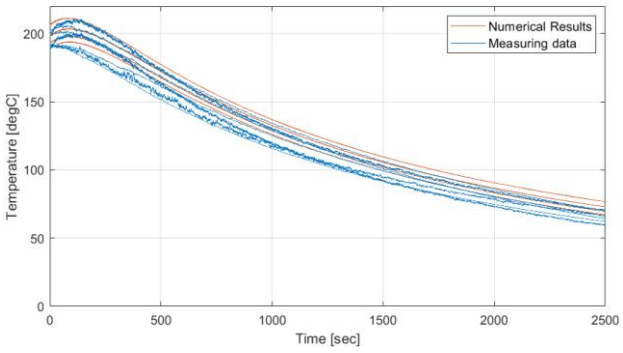

Fig. 17. Comparing the experimental and numerical results on case tube.

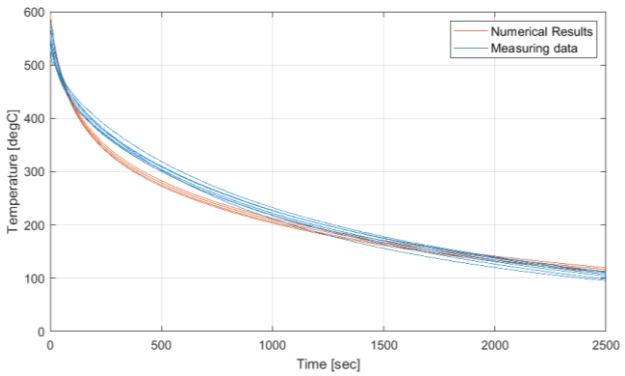

Fig. 18. Comparing the experimental and numerical results on middle tube.

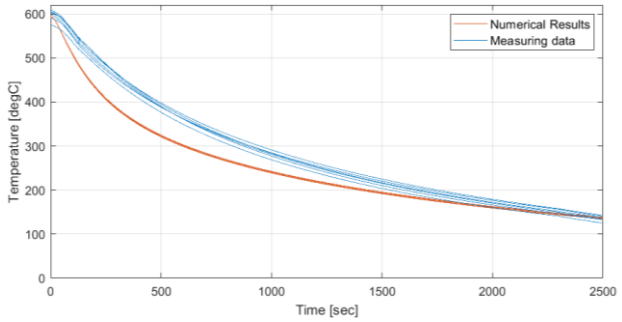

Fig. 19. Comparing the experimental and numerical results on shaft tube.

Based on the comparison, it can be concluded that the numerical and experimental results reach a good agreement.

The following Fig. 20 shows the percentage of heat transfer by radiation, convection and conduction from the outer tube. The individual heat transfer ratios are evaluated on the basis of a numerical calculation, where it can easily divide the partial heat transfer mechanism. The time dependence of the change in the mechanism of heat transfer from the dominant heat transfer by radiation to the stable method of heat transfer by radiation from 35% and heat transfer by convection 65% is shown. Heat transfer by conduction is negligible (less than 0.001%), as the computational model considers insulated walls and thus heat conduction is not significant. It is thus evident from the graphs on Fig. 20 that over time there is a greater effect of heat transfer by convection at the expense of radiation, this state stabilizes after 14 minutes at the 65%/35% ratio of radiation to convection. This is due to the temperature difference between the wall T_1 and the temperature of the surrounding air layer T_f seen in the equation Eq. 2,

$$q = \varepsilon \sigma_s \left(T_1 - T_f\right)^4. \quad (2)$$

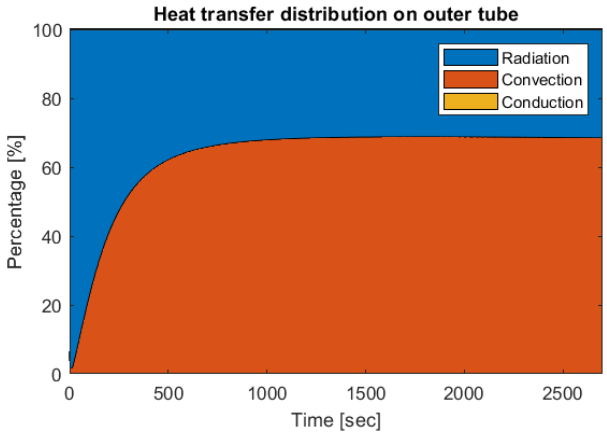

Fig. 20. Percentage of heat transfer on outer tube.

Finally, Fig. 21 shows the total heat flux through the outer tube where positive values indicate heat uptake from the environment and negative values indicate heat dissipation. The point of change of heat transfer from the direction of heat intake to heat outtake from the tube occurs after 4.5 min. At this point, heat transfer by radiation is no longer dominant, see Fig. 20.

This is followed by the point of maximum heat dissipation after 10.5 min. After this point, the system cools slowly until it cools down completely.

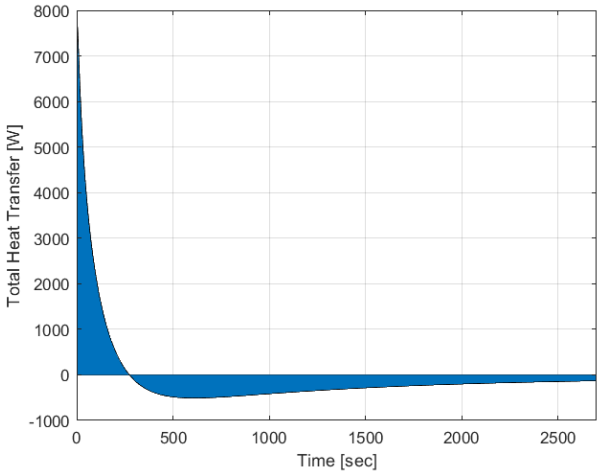

Fig. 21. Total heat transfer on outer tube.

4 Study of the middle tube influence

The verified numerical model was verified by experimental measurements on a specified middle tube. The following paragraph briefly describes the dependency of middle tube diameters on the temperature field parameters. The variable parameter of the middle tube diameter was determined and the solution for the selected steps of diameter changes was calculated. The variable parameter is related as the diameter of the middle tube to the diameter of the outer tube d / D = 0.5; 0.63 and 0.9. It is assumed that the initial conditions of the numerical model are identical to those when verifying the model on experimental data.

The aim of these calculations is to determine the change in the distribution of the temperature field of the system depending on the variable diameters of the

middle tube. The velocity distribution and the vortices are shown on the following Fig. 22 to Fig. 24.

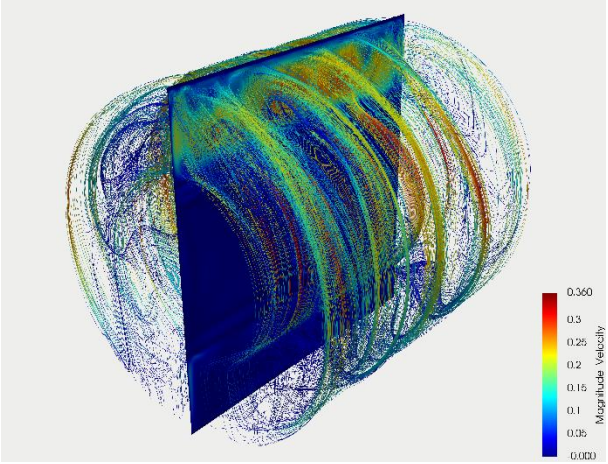

Fig. 22. The velocity field is plotted for the case d / D = 0.5.

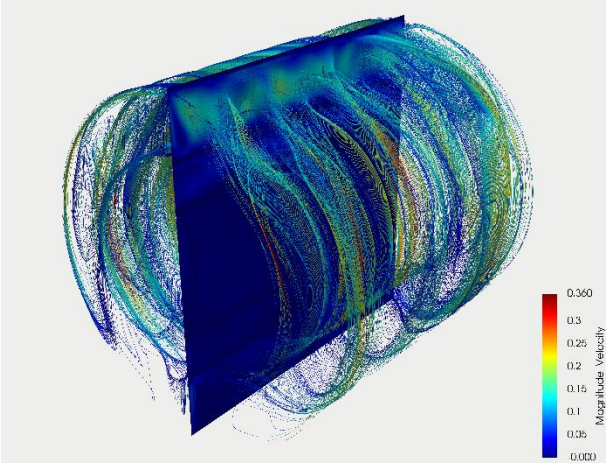

Fig. 23. The velocity field is plotted for the case d / D = 0.63.

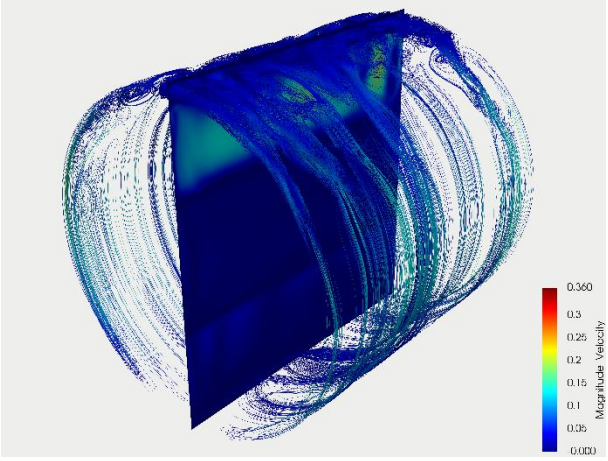

Fig. 24. The velocity field is plotted for the case d / D = 0.9.

Based on the figures shown above, it can be seen that the velocity field distribution changes with the changing size of the middle tube diameter. This results in a change in the temperature field and this affects the temperature difference between the top and bottom during cooling. When reducing the gap between the middle and outer tube, natural convection is not fully developed into one plume but into more plumes around the circumference. Furthermore, cooling with flowing hot air is not possible sufficiently rapidly, and thus cooling is slower.

Further, in Fig. 25 shows the iso-volumes of the velocity field on the initial case d / D = 0.63 from which is the steam the previously mentioned effect called the Rayleigh-Bénard Convection effect.

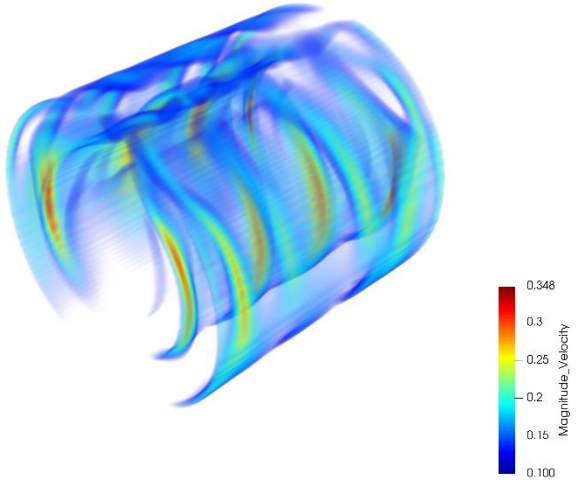

Fig. 25. Caption of the Figure 1. Below the figure.

From the above-described dependences of the velocity fields depending on the dimensions of the middle ring, it can be concluded that increasing the mean diameter has a positive effect on the consistency of the temperature field in the generator turbine section of the turboprop engine. By reducing the maximum values of the temperature difference between top and bottom, the effect of thermal expansion of the material is eliminated and thus the reduction of thermal deflection of the rotor parts of the motor is also called "Thermal Bow". This has a significant effect on the safety and trouble-free operation of the turbine engine during restart.

5 Conclusion

The results from the comparison of experimental data and the numerical model confirm the good accuracy of the numerical model. The suitability of the model used for the cooling analysis of the turboprop engine was confirmed and verified. This provides an effective tool for determining the non-stationary variable temperature field of a turboprop engine for stress analysis. The temperature-dependent deformation of a rotor assembly is called the “Rotor Thermal Bow” and will be studied in the following research. By predicting this phenomenon, it is possible to determine critical areas and conditions of thermal deflection. Contact between the stator and rotor part will be eliminated at the same time to maximize the efficiency of the turbine engine by reducing radial clearances.

Furthermore, the research will focus on the possibilities of influencing the temperature field. As already shown, the influence of the geometric characteristics of the middle tube or the influence of the flow will be studied.

Acknowledgment

Authors acknowledge support from the ESIF, EU Operational Programme Research, Development and Education, and from the Centre of Advanced Aerospace Technology (CZ.02.1.01/0.0/0.0/16_019/0000826), Faculty of Mechanical Engineering, Czech Technical University in Prague.

References

1. E. O. Smith and A. J. Neely. The impact of gas turbine compressor rotor bow on aircraft operations. The Aeronautical Journal. Royal Aeronautical Society, December 2017, **121**(1246), pp. 1808 - 1832. Available on: doi:10.1017/aer.2017.117
2. X. Yang and S. Kong. Numerical study of natural convection states in a horizontal concentric cylindrical annulus using SPH method. *Engineering Analysis with Boundary Elements*. December 2019, **2019**. Available on: doi:10.1016/j.enganabound.2019.02.007
3. P. T. Zubkov and E. I. Narygin. Numerical Study of Unsteady Natural Convection in a Horizontal Annular Channel. *Microgravity Science and Technology*. June 2020, **2020**(32), pp. 579 - 586. Available on: doi:10.1007/s12217-020-09791-2
4. E. Abu-Nada, Z. Masoud and A. Hijazi. Natural convection heat transfer enhancement in horizontal concentric annuli using nanofluids. *International Communications in Heat and Mass Transfer*. February 2008, **35**(2008), pp. 657 - 665. Available on: doi:10.1016/j.icheatmasstransfer.2007.11.004
5. N. Francis, S. Webb, M. Itamura and D. Janes. CFD Calculation of Internal Natural Convection in the Annulus Between Horizontal Concentric Cylinders. *International Communications in Heat and Mass Transfer*. Sandia National Laboratories, October 2002, (SAND2002-3132). Available on: doi:10.1115/HT2003-47515
6. Y. Wang, J. Chen and W. Zhang. Natural convection in a circular enclosure with an internal cylinder of regular polygon geometry. *AIP Advances 9*. June 2019, **065023**(2019). Available on: doi:10.1063/1.5100892
7. J. M. Prusa and L. Yao. Natural Convection Heat Transfer Between Eccentric Horizontal Cylinders. *Journal of Heat Transfer*. Lisbon, Portugal, February 1983, **105**(1), pp. 108 - 116. Available on: doi:10.1115/1.3245527
8. J. Pařez, P. Rohan and T. Vampola. Heat Transfer in Double Annular due to Natural Convection. *IOP Conference Series: Materials Science and Engineering*. Prague, Czech Republic, October 2021, **1190**(2021). Available on: doi:10.1088/1757-899X/1190/1/012002
9. E.L.M. Padilla and A. Silveira-Neto. Large-eddy simulation of transition to turbulence in natural convection in a horizontal annular cavity. International Journal of Heat and Mass Transfer. July 2008,**2008**(51). Available on: doi:10.1016/j.ijheatmasstransfer.2007.07.025
10. G. Krishnayatra, S. Tokas, R. Kumar and M. Zunaid. 3 Dimensional CFD analysis of Laminar flow Natural Convection of Hollow Cylinder with Annular Fins. *Proceedings of the 5th World Congress on Mechanical, Chemical, and Material Engineering*. Lisbon, Portugal, August 2019, (HTFF 181). Available on: doi:10.11159/htff19.181
11. S. Solnař, L. Popelka, M. Dostál, Cooling turboprop engine during shutdown. 13th International Conference on Experimental Fluid Mechanics (EFM 2018): EPJ Web of Conferences Volume 213, 2018. ISBN 9781510889668.
12. S. W. Churchill and H.S. Chu, Correlating equations for laminar and turbulent free convection from a horizontal cylinder, International Journal of Heat and Mass Transfer, 1975, Volume 18, Issue 9, pp- 1049-1053, ISSN 0017-9310,
13. R. B. Bird, W. E. Stewart and E. N. Ligthfoot. Transport Phenomena (John Wiley & Sons, Inc., New York / Chichester / Weinheim / Brisbane / Singapore / Toronto, 2002)
14. X. Yang and S. Kong. Numerical study of natural convection states in a horizontal concentric cylindrical annulus using SPH method. Engineering Analysis with Boundary Elements 2019. December 2019. Available on: doi:10.1016/j.enganabound.2019.02.007
15. M. P. King, M. Wilson and J. M. Owen. Rayleigh-Bénard Convection in Open and Closed Rotating Cavities. J. Eng. Gas Turbines Power [online]. April 2007, 129(2), pp. 305 - 311. Available on: doi:10.1115/1.2432898